

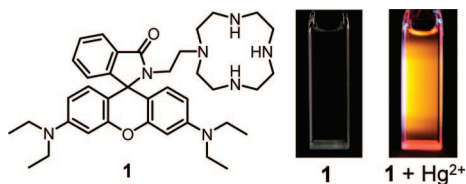
A Rhodamine–Cyclen Conjugate as a Highly Sensitive and Selective Fluorescent Chemosensor for Hg(II)

Yasuhiro Shiraishi,* Shigehiro Sumiya, Yoshiko Kohno, and Takayuki Hirai

Research Center for Solar Energy Chemistry, and Division of Chemical Engineering, Graduate School of Engineering Science, Osaka University, Toyonaka 560-8531, Japan

shiraish@cheng.es.osaka-u.ac.jp

Received June 09, 2008



A rhodamine–cyclen conjugate (**1**) behaves as a highly sensitive and selective fluorescent chemosensor for Hg²⁺. The high emission selectivity is due to the formation of 1–Hg²⁺ 1:2 complex leading to spirocycle opening of **1**.

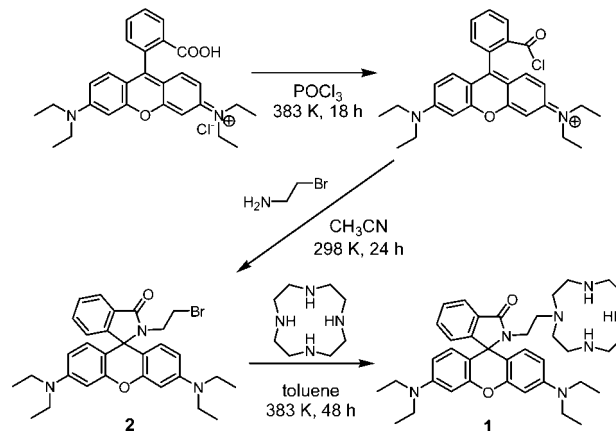
The design and development of fluorescent chemosensors for detection of biologically and environmentally important metal cations is currently of great importance, since they allow nondestructive and prompt detection of metal cations by a simple fluorescence enhancement (turn-on) or quenching (turn-off) response.¹ Hg²⁺ is one of the most hazardous components in the environment.² A large number of fluorescent chemosensors for Hg²⁺ have therefore been proposed so far. Most of these sensors, however, show fluorescence quenching (turn-off) response,³ and the sensors with fluorescence enhancement (turn-on) response are still rare.⁴

(1) For books and reviews: (a) Czarnik, A. W. *Fluorescent Chemosensors for Ion and Molecule Recognition*; American Chemical Society: Washington DC, 1993. (b) de Silva, A. P.; Gunaratne, H. Q. N.; Gunnlaugsson, T.; Huxley, A. J. M.; McCoy, C. P.; Rademacher, J. T.; Rice, T. E. *Chem. Rev.* **1997**, *97*, 1515–1566. (c) Valeur, B.; Leray, I. *Coord. Chem. Rev.* **2000**, *205*, 3–40. (d) Martínez-Máñez, R.; Sancenón, F. *Chem. Rev.* **2003**, *103*, 4419–4476. (e) Callan, J. F.; de Silva, A. P.; Magri, D. C. *Tetrahedron* **2005**, *61*, 8551–8588. (f) Basabe-Desmonts, L.; Reinhoudt, D. N.; Crego-Calama, M. *Chem. Soc. Rev.* **2007**, *36*, 993–1017.

(2) Boening, D. W. *Chemosphere* **2000**, *40*, 1335–1351.

(3) (a) Ono, A.; Togashi, H. *Angew. Chem., Int. Ed.* **2004**, *43*, 4300–4302. (b) Moon, S.-Y.; Youn, N. J.; Park, S. M.; Chang, S.-K. *J. Org. Chem.* **2005**, *70*, 2394–2397. (c) Ha-Thi, M.-H.; Penhoat, M.; Michelet, V.; Leray, I. *Org. Lett.* **2007**, *9*, 1133–1136. (d) Praveen, L.; Ganga, V. B.; Thirumalai, R.; Sreeja, T.; Reddy, M. L. P.; Varma, R. L. *Inorg. Chem.* **2007**, *46*, 6277–6282.

SCHEME 1. Synthesis of Rhodamine–Cyclen Conjugate, **1**



Rhodamine is a dye used extensively as a fluorescence labeling reagent due to its excellent photophysical properties, such as long absorption and emission wavelengths, large absorption coefficient, and high fluorescence quantum yield.⁵ Recently, various rhodamine-based turn-on fluorescent Hg²⁺ sensors have been proposed.⁶ The Hg²⁺ sensing mechanism of these sensors is based on the change in structure between the spirocyclic and open-cycle forms. Without Hg²⁺, these sensors exist in a nonemissive spirocyclic form. Addition of Hg²⁺ leads to reversible coordination with the ligand groups, resulting in spirocycle opening along with an appearance of orange fluorescence and a clear color change from colorless to pink. These Hg²⁺ sensors, however, show insufficient sensitivity (emission enhancement factor is <1000) and insufficient emission selectivity to Hg²⁺ (emission intensity obtained with Hg²⁺ is less than 20 times of that obtained with other metal cation).

Cyclen (1,4,7,10-tetraazacyclododecane) is one of the most extensively studied ligands and can coordinate strongly with many transition metal cations.⁷ Herein we report a rhodamine–cyclen

(4) (a) Guo, X.; Qian, X.; Jia, L. *J. Am. Chem. Soc.* **2004**, *126*, 2272–2273. (b) Zhang, H.; Han, L.-F.; Zachariasse, K. A.; Jiang, Y.-B. *Org. Lett.* **2005**, *7*, 4217–4220. (c) Avirah, R. R.; Jyothish, K.; Ramaiah, D. *Org. Lett.* **2007**, *9*, 121–124. (d) Yoon, S.; Miller, E. W.; He, Q.; Do, P. H.; Chang, C. *J. Angew. Chem., Int. Ed.* **2007**, *46*, 6658–6661. (e) Shiraishi, Y.; Maehara, H.; Ishizumi, K.; Hirai, T. *Org. Lett.* **2007**, *9*, 3125–3128.

(5) Lakowicz, J. R. *Principles of Fluorescence Spectroscopy*, 3rd ed.; Springer: New York, 2006; pp 67–69.

(6) (a) Zheng, H.; Qian, Z.-H.; Xu, L.; Yuan, F.-F.; Lan, L.-D.; Xu, J.-G. *Org. Lett.* **2006**, *8*, 859–861. (b) Lee, M. H.; Wu, J.-S.; Lee, J. W.; Jung, J. H.; Kim, J. S. *Org. Lett.* **2007**, *9*, 2501–2504. (c) Yang, H.; Zhou, Z.; Huang, K.; Yu, M.; Li, F.; Yi, T.; Huang, C. *Org. Lett.* **2007**, *9*, 4729–4732. (d) Wu, D.; Huang, W.; Duan, C.; Lin, Z.; Meng, Q. *Inorg. Chem.* **2007**, *46*, 1538–1540. (e) Soh, J. H.; Swamy, K. M. K.; Kim, S. K.; Kim, S.; Lee, S.-H.; Yoon, J. *Tetrahedron Lett.* **2007**, *48*, 5966–5969.

(7) (a) Aoki, S.; Zulkofeli, M.; Shiro, M.; Kohsako, M.; Takeda, K.; Kimura, E. *J. Am. Chem. Soc.* **2005**, *127*, 9129–9139. (b) Aoki, S.; Kagata, D.; Shiro, M.; Takeda, K.; Kimura, E. *J. Am. Chem. Soc.* **2004**, *126*, 13377–13390. (c) Koike, T.; Watanabe, T.; Aoki, S.; Kimura, E.; Shiro, M. *J. Am. Chem. Soc.* **1996**, *118*, 12696–12703. (d) Aoki, S.; Sakurama, K.; Ohshima, R.; Matsuo, N.; Yamada, Y.; Takasawa, R.; Tanuma, S.-i.; Takeda, K.; Kimura, E. *Inorg. Chem.* **2008**, *47*, 2747–2754. (e) Amorim, M. T. S.; Chaves, S.; Delgado, R.; da Silva, J. J. R. F. *J. Chem. Soc., Dalton Trans.* **1991**, *11*, 3065–3072.

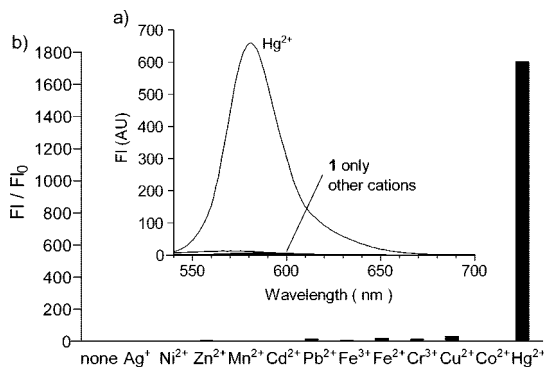


FIGURE 1. (a) Fluorescence spectra ($\lambda_{\text{ex}} = 530 \text{ nm}$) of **1** ($50 \mu\text{M}$) measured in CH_3CN with respective metal cations (10 equiv). (b) Fluorescence enhancement factor of **1**, where FI and FI_0 are the fluorescence intensity at 580 nm measured with and without metal cations (10 equiv). Absorption spectra of **1** obtained with respective metal cations are shown in Figure S1 (Supporting Information).

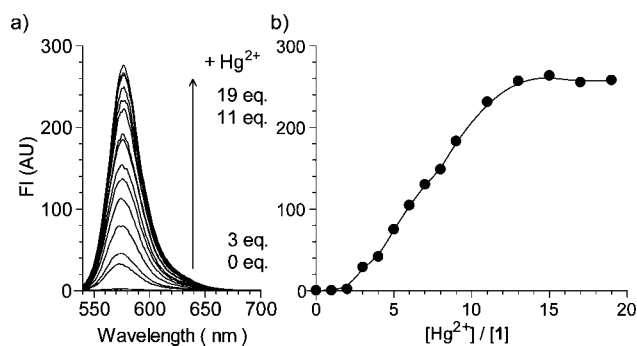


FIGURE 2. (a) Change in fluorescence spectra ($\lambda_{\text{ex}} = 530 \text{ nm}$) of **1** ($5 \mu\text{M}$) measured in CH_3CN upon addition of Hg^{2+} . (b) Change in fluorescence intensity at 580 nm. Fluorescence titration result of compound **2** is shown in Figure S2 (Supporting Information), where almost no emission enhancement is observed.

conjugate (**1**, Scheme 1) that behaves as a fluorescent Hg^{2+} sensor with high emission sensitivity and selectivity. We describe here that the high emission selectivity of **1** to Hg^{2+} is due to the selective formation of **1**– Hg^{2+} 1:2 complex.

The synthesis of **1** is shown in Scheme 1 (see the Experimental Section). Reaction of rhodamine B hydrochloride with POCl_3 followed by 2-bromoethylamine hydrobromide affords the compound **2** with 21% yield. Reaction of compound **2** with cyclen affords **1** with 86% yield.

Figure 1a shows fluorescence spectra ($\lambda_{\text{ex}} = 530 \text{ nm}$) of **1** ($50 \mu\text{M}$) measured in CH_3CN with respective metal cations (10 equiv). Without cations, **1** shows very weak fluorescence. Addition of Hg^{2+} , however, creates strong orange fluorescence at 540–670 nm (see the abstract graphic). As shown in Figure 1b, the fluorescence enhancement factor measured at 580 nm with 10 equiv of Hg^{2+} is determined to be 1700, which is the highest value among the early reported rhodamine-based Hg^{2+} sensors.⁶ In contrast, addition of other metal cations scarcely shows fluorescence enhancement. The fluorescence enhancement factor of Hg^{2+} is more than 50 times of that obtained with other metal cations and is much higher than that obtained with the early reported rhodamine-based Hg^{2+} sensors (<20 times).⁶ These findings indicate that **1** behaves as a highly sensitive and selective fluorescent Hg^{2+} sensor.

Figure 2 shows the result of fluorescence titration of **1** with Hg^{2+} . The Hg^{2+} addition leads to increase in the 580 nm fluorescence and the increase is saturated upon addition of 15

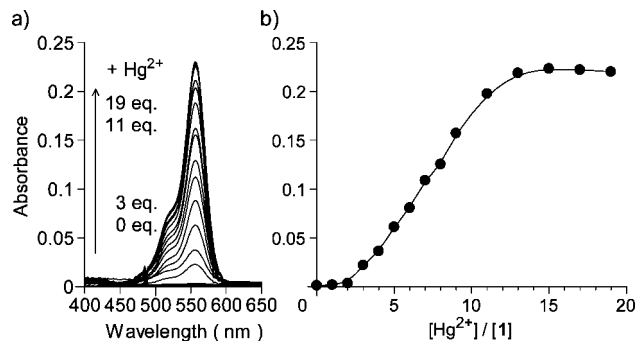


FIGURE 3. (a) Change in absorption spectra of **1** ($5 \mu\text{M}$) measured in CH_3CN upon addition of Hg^{2+} . (b) Change in 558 nm absorbance.

equiv of Hg^{2+} .⁸ The fluorescence increase occurs immediately upon Hg^{2+} addition and is saturated within 1 min. Figure 3a shows change in absorption spectra of **1**. Without Hg^{2+} , **1** scarcely shows absorption at 450–600 nm, indicating that **1** exists as a spirocyclic form.⁶ Addition of Hg^{2+} , however, shows a distinctive absorption at 450–600 nm, along with a clear color change from colorless to pink. As shown in Figure 3b, the absorption increase is saturated upon addition of 15 equiv of Hg^{2+} , which is similar to the fluorescence titration result (Figure 2b).

Addition of triethylenetetramine to a solution containing **1** and Hg^{2+} leads to immediate disappearance of both pink color and orange fluorescence. This indicates that **1** reversibly coordinates with Hg^{2+} . The Hg^{2+} -induced coloration and emission of **1** are therefore explained by the reversible coordination of **1** with Hg^{2+} leading to spirocycle opening of **1**, as is the case for related rhodamine-based sensors.⁶

1 coordinates with Hg^{2+} in a 1:2 stoichiometry. This is confirmed by the Benesi–Hildebrand method.⁹ When assuming a 1:2 association between **1** and Hg^{2+} , the Benesi–Hildebrand equation is given as follows (see the Supporting Information):

$$\frac{1}{A - A_0} = \frac{1}{K(A_{\text{max}} - A_0)[\text{Hg}^{2+}]_0^2} + \frac{1}{A_{\text{max}} - A_0} \quad (1)$$

A_0 is the absorbance of **1**, A is the absorbance obtained with Hg^{2+} , A_{max} is the absorbance obtained with excess amount of Hg^{2+} , K is the association constant (M^{-2}), and $[\text{Hg}^{2+}]_0$ is the concentration of Hg^{2+} added (M). As shown in Figure 4, the plot of $1/(A - A_0)$ against $1/[\text{Hg}^{2+}]_0^2$ shows a linear relationship, indicating that **1** indeed associates with Hg^{2+} in a 1:2 stoichiometry. The association constant, K , between **1** and two Hg^{2+} , is determined from the slope to be $2.3 \times 10^8 \text{ M}^{-2}$. The 1:2 complex formation is also confirmed by ESI-MS analysis: a CH_3CN solution containing **1** and 6 equiv of $\text{Hg}(\text{CF}_3\text{SO}_3)_2$ (Figure S5, Supporting Information) shows a strong peak at m/z 1487.3, assigned to $[\text{2Hg}^{2+} + \text{1} + 3\text{CF}_3\text{SO}_3]^{+}$ ion, indicating that **1** actually forms 1:2 complex.

It is well-known that cyclen coordinates with one metal cation;⁷ however, the above experimental results indicate that the spirocycle opening of **1** requires two Hg^{2+} . This means that coordination of one Hg^{2+} does not lead to spirocycle opening.

(8) The fluorescence quantum yield (Φ_{F}) of **1** with 15 equiv of Hg^{2+} is determined to be 0.19, based on rhodamine B standard ($\Phi_{\text{F}} = 0.69$ in ethanol): (a) Parker, C. A.; Rees, W. T. *Analyst* **1960**, *85*, 587–600.

(9) (a) Benesi, H. A.; Hildebrand, J. H. *J. Am. Chem. Soc.* **1949**, *71*, 2703–2707. (b) Yang, C.; Liu, L.; Mu, T.-W.; Guo, Q.-X. *Anal. Sci.* **2000**, *16*, 537–539. (c) Rodríguez-Cáceres, M. I.; Agbaria, R. A.; Warner, I. M. *J. Fluoresc.* **2005**, *15*, 185–190.

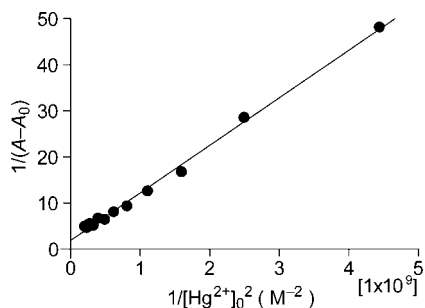


FIGURE 4. Benesi–Hildebrand plot (558 nm absorbance) of **1** using eq. 1, assuming 1:2 stoichiometry for association between **1** and Hg^{2+} . The plot assuming 1:1 stoichiometry is shown in Figure S3 (Supporting Information) for comparison.

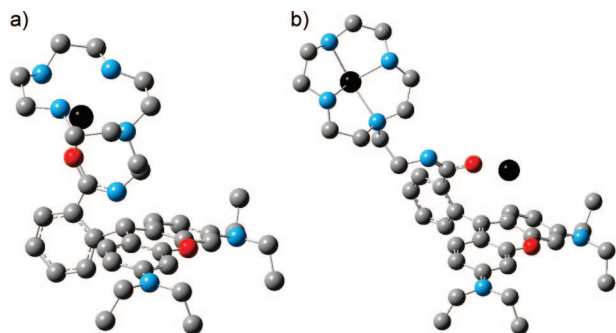


FIGURE 5. Calculated structures of (a) 1:1 and (b) 1:2 **1**– Hg^{2+} complexes (B3LYP/6-31G* with the Stuttgart Relativistic Small-Core basis set for Hg atom with effective core potential). Gray, blue, red, and black atoms denote C, N, O, and Hg atoms, respectively, where H atoms are omitted for clarity.

and coordination of second Hg^{2+} does. To clarify the coordination geometry of **1** and Hg^{2+} , ab initio calculations were performed with the Gaussian 03 program,^{4e,10,11} at the DFT level with B3LYP/6-31G*, with the Stuttgart Relativistic Small-Core basis set for Hg with effective core potential.¹² Figure 5a shows optimized geometry of nonemissive **1**– Hg^{2+} 1:1 complex. Hg^{2+} is coordinated with four cyclen nitrogens and carbonyl oxygen of **1**. In the case of related rhodamine-based Hg^{2+} sensors,⁶ nucleophilic coordination of carbonyl oxygen to Hg^{2+} leads to spirocycle opening. No spirocycle opening of the 1:1 complex is probably due to the weak coordination of the carbonyl oxygen

(10) Gaussian 03, Revision B.05: Frisch, M. J.; Trucks, G. W.; Schlegel, H. B.; Scuseria, G. E.; Robb, M. A.; Cheeseman, J. R.; Montgomery, Jr., J. A.; Vreven, T.; Kudin, K. N.; Burant, J. C.; Millam, J. M.; Iyengar, S. S.; Tomasi, J.; Barone, V.; Mennucci, B.; Cossi, M.; Scalmani, G.; Rega, N.; Petersson, G. A.; Nakatsuji, H.; Hada, M.; Ehara, M.; Toyota, K.; Fukuda, R.; Hasegawa, J.; Ishida, M.; Nakajima, T.; Honda, Y.; Kitao, O.; Nakai, H.; Klene, M.; Li, X.; Knox, J. E.; Hratchian, H. P.; Cross, J. B.; Bakken, V.; Adamo, C.; Jaramillo, J.; Gomperts, R.; Stratmann, R. E.; Yazyev, O.; Austin, A. J.; Cammi, R.; Pomelli, C.; Ochterski, J. W.; Ayala, P. Y.; Morokuma, K.; Voth, G. A.; Salvador, P.; Dannenberg, J. J.; Zakrzewski, V. G.; Dapprich, S.; Daniels, A. D.; Strain, M. C.; Farkas, O.; Malick, D. K.; Rabuck, A. D.; Raghavachari, K.; Foresman, J. B.; Ortiz, J. V.; Cui, Q.; Baboul, A. G.; Clifford, S.; Cioslowski, J.; Stefanov, B. B.; Liu, G.; Liashenko, A.; Piskorz, P.; Komaromi, I.; Martin, R. L.; Fox, D. J.; Keith, T.; Al-Laham, M. A.; Peng, C. Y.; Nanayakkara, A.; Challacombe, M.; Gill, P. M. W.; Johnson, B.; Chen, W.; Wong, M. W.; Gonzalez, C.; Pople, J. A. Gaussian, Inc.: Wallingford CT, 2004.

(11) Shiraishi, Y.; Ichimura, C.; Hirai, T. *Tetrahedron Lett.* **2007**, *48*, 7769–7773.

(12) The basis set was obtained from the Extensible Computational Chemistry Environment Basis Set Database, Version 02/02/06, as developed and distributed by the Molecular Science Computing Facility, Environmental and Molecular Sciences Laboratory which is part of the Pacific Northwest Laboratory, P.O. Box 999, Richland, WA 99352, and funded by the U.S. Department of Energy. The Pacific Northwest Laboratory is a multiprogram laboratory operated by Battelle Memorial Institute for the U.S. Department of Energy under contract DE-AC06-76RLO 1830.

with Hg^{2+} . The positive charge of the Hg^{2+} atom is significantly decreased by strong coordination with the cyclen nitrogens.¹³ This probably leads to weak coordination of the carbonyl oxygen with Hg^{2+} , resulting in no spirocycle opening.

Figure 5b shows optimized geometry of the emissive 1:2 **1**– Hg^{2+} complex. The first Hg^{2+} atom remains within the cyclen moiety, but the carbonyl oxygen is detached and coordinates with second Hg^{2+} . The coordination of the carbonyl oxygen with the second Hg^{2+} , therefore, leads to spirocycle opening of **1**. The distance between the second Hg^{2+} and the xanthene plane of **1** is determined to be $<2.5 \text{ \AA}$, which is much shorter than the sum of the van der Waals radii of Hg and C (3.43 \AA).¹⁴ This indicates that the second Hg^{2+} is stabilized by the coordination with the carbonyl oxygen and the cation– π interaction with the xanthene moiety.^{4e,15,16}

The high emission selectivity of **1** to Hg^{2+} (Figure 1) is due to the formation of 1:2 complex, where other metal cations forms nonemissive 1:1 complexes. This is confirmed by ESI mass analysis of **1** with other cations. It is well-known that Cu^{2+} and Pb^{2+} also coordinate strongly with cyclen, although the binding constant is lower than that of Hg^{2+} .¹⁷ The mass charts of **1** measured with these cations show a distinctive peak assigned to the 1:1 complexes (Figures S6 and S7, Supporting Information).¹⁸ These cations coordinate with cyclen nitrogens more weakly than does Hg^{2+} ,¹⁷ therefore, the positive charge on these cations is higher. This may allow stronger coordination of the carbonyl oxygen with these cations and, hence, suppresses the 1:2 complex formation, resulting in no spirocycle opening. The high emission selectivity of **1** to Hg^{2+} (Figure 1) is therefore due to the strong Hg^{2+} –cyclen binding, allowing coordination of the carbonyl oxygen with second Hg^{2+} .

IR titration of **1** in CH_3CN confirm the proposed mechanism. As shown in Figure 6b, i and ii, carbonyl absorption of **1** (1686.9 cm^{-1}) shifts to lower frequency (1632.5 cm^{-1}) upon addition of 1 equiv of Cu^{2+} , indicating that carbonyl oxygen indeed coordinates with Cu^{2+} .¹⁹ In contrast, as shown in Figure 6a, i and ii, addition of 1 equiv of Hg^{2+} scarcely changes the absorption. This indicates that coordination of carbonyl oxygen with the first Hg^{2+} is weaker than that with Cu^{2+} . As shown in

(13) (a) Nakamoto, K. *Infrared and Raman Spectra of Inorganic and Coordination Compounds*; John Wiley & Sons: New York, 1962; p 261. (b) Rodríguez-Hernández, J.; Reguera, E.; Lima, E.; Balmaseda, J.; Martínez-García, R.; Yee-Madeira, H. *J. Phys. Chem. Solids* **2007**, *68*, 1630–1642.

(14) (a) Canty, A. J.; Chaichit, N.; Gatehouse, B. M.; George, E. E. *Inorg. Chem.* **1981**, *20*, 4293–4300. (b) Batsanov, S. S. *Inorg. Mater.* **2001**, *37*, 871–885.

(15) (a) Kang, J.; Choi, M.; Kwon, J. Y.; Lee, E. Y.; Yoon, J. *J. Org. Chem.* **2002**, *67*, 4384–4386. (b) Iyoda, M.; Kuwatani, Y.; Yamauchi, T.; Oda, M. *J. Chem. Soc., Chem. Commun.* **1988**, 65–66. (c) Pierre, J.-L.; Baret, P.; Chautemps, P.; Armand, M. *J. Am. Chem. Soc.* **1981**, *103*, 2986–2988. (d) Heitzler, F. R.; Hopf, H.; Jones, P. G.; Bubenitschek, P.; Lehne, V. *J. Org. Chem.* **1993**, *58*, 2781–2784. (e) Burress, C. N.; Bodine, M. I.; Elbjeirami, O.; Reibenspies, J. H.; Omary, M. A.; Gabbai, F. P. *Inorg. Chem.* **2007**, *46*, 1388–1395.

(16) ¹H NMR titration of **1** with Hg^{2+} (Figure S4, Supporting Information) does not show characteristic spectrum change with the Hg^{2+} amount. This is because coordination of first Hg^{2+} with cyclen moiety strongly affects the electron density of **1**; therefore, the effect of second $Hg(II)$ coordination via cation– π interaction becomes negligibly small.

(17) (a) Kodama, M.; Kimura, E. *J. Chem. Soc., Dalton Trans.* **1977**, 2269–2276. (b) Amorim, M. T. S.; Chaves, S.; Delgado, R.; da Silva, J. J. R. *J. Chem. Soc., Dalton Trans.* **1991**, 3065–3072. (c) Kodama, M.; Kimura, E. *J. Chem. Soc., Dalton Trans.* **1978**, 1081–1085.

(18) As shown in Figure S8 (Supporting Information), the optimized geometry of **1**– Cu^{2+} 1:1 complex is similar to that of **1**– Hg^{2+} 1:1 complex, indicating that these cations (Cu^{2+} , Pb^{2+}) coordinates with cyclen and carbonyl oxygen, as is also the case for **1**– Hg^{2+} 1:1 complex (Figure 5a).

(19) (a) Zhang, X.; Shiraishi, Y.; Hirai, T. *Org. Lett.* **2007**, *9*, 5039–5042. (b) Kwon, J. Y.; Jang, Y. J.; Lee, Y. J.; Kim, K. M.; Seo, M. S.; Nam, W.; Yoon, J. *J. Am. Chem. Soc.* **2005**, *127*, 10107–10111.

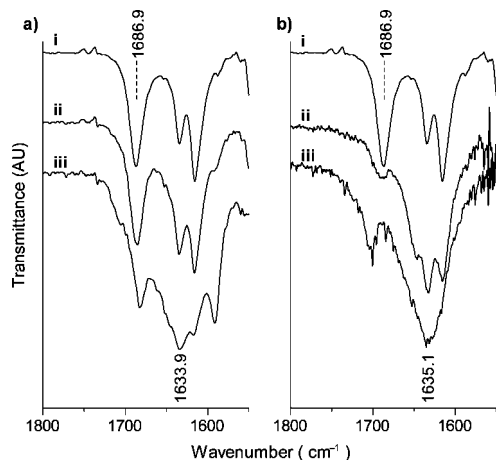


FIGURE 6. IR spectra of **1** (10 mM) measured in CH_3CN with (a) Hg^{2+} and (b) Cu^{2+} : (i) without cations, (ii) with 1 equiv of cation, and (iii) with 4 equiv of cation.

Figure 6a, iii, addition of 4 equiv of Hg^{2+} leads to shift of the carbonyl absorption to lower frequency (1633.9 cm^{-1}).^{6b,20} These findings clearly supports the ring-opening mechanism: the carbonyl oxygen of **1** binds very weakly with the first Hg^{2+} , but coordinates strongly with second Hg^{2+} , leading to spirocycle opening.

In summary, we found that a rhodamine–cyclen conjugate (**1**) behaves as a highly sensitive and selective fluorescent Hg^{2+} sensor. The high emission selectivity of **1** to Hg^{2+} is simply driven by the selective formation of 1:2 complex. Although **1** works only in organic media²¹ and the detailed mechanism of the Hg^{2+} -selective emission remains to be clarified, the molecular design presented here may contribute to the development of more efficient and more useful chemosensors based on the rhodamine platform.

Experimental Section

General Methods. Perchlorate (Hg^{2+} , Cu^{2+} , Zn^{2+} , Cd^{2+} , Pb^{2+} , Cr^{3+} , Mn^{2+} , Fe^{2+} , Fe^{3+}), nitrate (Ni^{2+} , Co^{2+}), and tetrafluoroborate salts (Ag^+) were used as the metal cation source. Apparatus and instruments were described elsewhere.²² The measurements were carried out with 10-mm path length Pyrex cell under air.

(20) Zhang, X.; Shiraishi, Y.; Hirai, T. *Tetrahedron Lett.* **2007**, *48*, 5455–5459.

(21) The fluorescence intensity of **1**, when measured with 10 equiv of Hg^{2+} in CH_3CN containing water up to 0.2%, is similar to that obtained without water; however, 30% and 100% intensity reductions occur in the presence of 0.3% and 0.4% water, respectively.

(22) (a) Nishimura, G.; Maehara, H.; Shiraishi, Y.; Hirai, T. *Chem.—Eur. J.* **2008**, *14*, 259–271. (b) Shiraishi, Y.; Miyamoto, R.; Zhang, X.; Hirai, T. *Org. Lett.* **2007**, *9*, 3921–3924. (c) Shiraishi, Y.; Miyamoto, R.; Hirai, T. *Langmuir* **2008**, *24*, 4273–4279.

Compound 2. Rhodamine B hydrochloride (1.0 g, 2 mmol) was refluxed in POCl_3 (5 mL) for 18 h and concentrated by evaporation. The obtained crude acid chloride was dissolved in CH_3CN (10 mL) together with 2-bromoethylamine hydrobromide (1.0 g, 5 mmol) and triethylamine (1 mL) and stirred at room temperature for 24 h under N_2 . The resultant was concentrated by evaporation. Water was added to the residue, and the aqueous phase was extracted with CH_2Cl_2 (20 mL \times 2). The organic layer was washed with water, dried over Na_2SO_4 , and concentrated by evaporation. The crude product was purified by silica gel column chromatography with $\text{CH}_2\text{Cl}_2/\text{CH}_3\text{OH}$ (100/1 v/v), affording **2** as a pale pink solid (0.24 g, 21%). ^1H NMR (CDCl_3 , 270 MHz, TMS): δ (ppm) = 1.17 (t, 12H, $J = 7.01$ Hz), 3.00 (t, 2H, $J = 8.17$ Hz), 3.34 (q, 8H, $J = 7.04$ Hz), 3.52 (t, 2H, $J = 8.25$ Hz), 6.25–6.44 (m, 6H), 7.05–7.08 (m, 1H), 7.42–7.45 (m, 2H), 7.88–7.92 (m, 1H). ^{13}C NMR (CDCl_3 , 100 MHz): δ (ppm) = 16.1, 29.2, 31.7, 52.1, 85.2, 92.5, 95.5, 110.2, 111.1, 115.3, 115.9, 117.9, 119.9, 136.2, 140.5, 140.8, 155.2. FAB-MS: calcd for $\text{C}_{30}\text{H}_{34}\text{N}_3\text{O}_2\text{Br}$ 548.5, found m/z 548.2 (M^+). ^1H , ^{13}C NMR and FAB-MS charts are shown in Figure S9–S11 (Supporting Information).

Compound 1. Compound **2** (0.24 g, 0.4 mmol) and cyclen (0.50 g, 2.91 mmol) were refluxed in toluene (40 mL) for 48 h under dry N_2 . The resulting solution was concentrated by evaporation and dissolved in ethanol (5 mL). Concentrated HCl was added to the solution, and the precipitated HCl salt of the unreacted cyclen was removed by filtration. The residue was concentrated by evaporation, dissolved in water (10 mL), and washed with CHCl_3 . An aqueous NaOH solution (5 M, 15 mL) was added to the solution and extracted with CH_2Cl_2 (10 mL \times 5). The organic layer was dried over Na_2SO_4 and concentrated by evaporation. The residue was dried in vacuo at 353 K for 8 h, affording **1** as a yellow powder (0.58 g, 86%). ^1H NMR (CDCl_3 , 270 MHz, TMS): δ (ppm) = 1.16 (t, 12H, $J = 7.01$ Hz), 2.23–2.29 (m, 2H), 2.40–2.73 (m, 16H), 3.19–3.25 (m, 2H), 3.34 (q, 8H, $J = 7.04$ Hz), 6.24–6.43 (m, 6H), 7.04–7.07 (m, 1H), 7.37–7.42 (m, 2H), 7.85–7.88 (m, 1H). ^{13}C NMR (CDCl_3 , 68 MHz): δ (ppm) = 12.6, 37.9, 44.3, 45.4, 46.3, 47.2, 51.3, 52.2, 64.8, 97.8, 105.7, 108.0, 122.4, 123.6, 127.7, 128.7, 131.3, 132.0, 148.6, 153.2, 167.4. FAB-MS: calcd for $\text{C}_{38}\text{H}_{53}\text{N}_7\text{O}_2$ 639.8, found m/z 640.7 ($\text{M} + \text{H}^+$). Anal. Calcd: C, 71.32; H, 8.35; N, 15.32. Found: C, 70.74; H, 8.03; N, 14.75. ^1H , ^{13}C NMR and FAB-MS charts are shown in Figures S12–S14 (Supporting Information).

Acknowledgment. This work was supported by Grant-in-Aids for Scientific Research (No. 19760536) from the Ministry of Education, Culture, Sports, Science and Technology, Japan (MEXT).

Supporting Information Available: Benesi–Hildebrand equation for 1:2 association, Figures S1–S14, and Cartesian coordinates for respective compounds. This material is available free of charge via the Internet at <http://pubs.acs.org>.

JO8012447